



UNIVERSITY OF LEEDS

This is a repository copy of *Optical properties of tissue measured using terahertz pulsed imaging..*

White Rose Research Online URL for this paper:
<http://eprints.whiterose.ac.uk/761/>

Article:

Berry, E., Fitzgerald, A.J., Zinov'ev, N.N. et al. (6 more authors) (2003) Optical properties of tissue measured using terahertz pulsed imaging. *Proceedings of SPIE: Medical Imaging 2003: Physics of Medical Imaging*, 5030. pp. 459-470. ISSN 1605-7422

<https://doi.org/10.1117/12.479993>

Reuse

See Attached

Takedown

If you consider content in White Rose Research Online to be in breach of UK law, please notify us by emailing eprints@whiterose.ac.uk including the URL of the record and the reason for the withdrawal request.



eprints@whiterose.ac.uk
<https://eprints.whiterose.ac.uk/>



White Rose
university consortium
Universities of Leeds, Sheffield & York

White Rose Consortium ePrints Repository

<http://eprints.whiterose.ac.uk/>

This is an author produced version of a paper published in **Proceedings of SPIE: Medical Imaging 2003**. This paper has been peer-reviewed but does not include the final publisher journal pagination.

White Rose Repository URL for this paper:
<http://eprints.whiterose.ac.uk/archive/00000761/>

Citation for the published paper

Berry, E. and Fitzgerald, A.J. and Zinov'ev, N.N. and Walker, G.C. and Homer-Vanniasinkam, S. and Sudworth, C.D. and Miles, R.E. and Chamberlain, J.M. and Smith, M.A. (2003) *Optical properties of tissue measured using terahertz pulsed imaging*. Proceedings of SPIE: Medical Imaging 2003: Physics of Medical Imaging, 5030. pp. 459-470.

Citation for this paper

To refer to the repository paper, the following format may be used:

Berry, E. and Fitzgerald, A.J. and Zinov'ev, N.N. and Walker, G.C. and Homer-Vanniasinkam, S. and Sudworth, C.D. and Miles, R.E. and Chamberlain, J.M. and Smith, M.A. (2003) *Optical properties of tissue measured using terahertz pulsed imaging*. Author manuscript available at:

[<http://eprints.whiterose.ac.uk/archive/00000761/>] [Accessed: *date*].

Published in final edited form as:

Berry, E. and Fitzgerald, A.J. and Zinov'ev, N.N. and Walker, G.C. and Homer-Vanniasinkam, S. and Sudworth, C.D. and Miles, R.E. and Chamberlain, J.M. and Smith, M.A. (2003) *Optical properties of tissue measured using terahertz pulsed imaging*. Proceedings of SPIE: Medical Imaging 2003: Physics of Medical Imaging, 5030. pp. 459-470.

Optical properties of tissue measured using terahertz pulsed imaging

Elizabeth Berry^a, Anthony J. Fitzgerald^a, Nickolay N. Zinov'ev^b, Gillian C. Walker^a,
Shervanthi Homer-Vanniasinkam^c, Caroline D. Sudworth^a, Robert E. Miles^b,
J. Martyn Chamberlain^b, Michael A. Smith^a

^a Academic Unit of Medical Physics and Centre of Medical Imaging Research, University of Leeds;

^b School of Electronic and Electrical Engineering, University of Leeds; ^c Vascular Surgical Unit,
Leeds Teaching Hospitals NHS Trust, Leeds.

ABSTRACT

The first demonstrations of terahertz imaging in biomedicine were made several years ago, but few data are available on the optical properties of human tissue at terahertz frequencies. A catalogue of these properties has been established to estimate variability and determine the practicality of proposed medical applications in terms of penetration depth, image contrast and reflection at boundaries. A pulsed terahertz imaging system with a useful bandwidth 0.5-2.5 THz was used. Local ethical committee approval was obtained. Transmission measurements were made through tissue slices of thickness 0.08 to 1 mm, including tooth enamel and dentine, cortical bone, skin, adipose tissue and striated muscle. The mean and standard deviation for refractive index and linear attenuation coefficient, both broadband and as a function of frequency, were calculated. The measurements were used in simple models of the transmission, reflection and propagation of terahertz radiation in potential medical applications. Refractive indices ranged from 1.5 ± 0.5 for adipose tissue to 3.06 ± 0.09 for tooth enamel. Significant differences ($P < 0.05$) were found between the broadband refractive indices of a number of tissues. Terahertz radiation is strongly absorbed in tissue so reflection imaging, which has lower penetration requirements than transmission, shows promise for dental or dermatological applications.

Keywords: refractive index, linear absorption coefficient, human tissue, terahertz pulsed imaging, medical applications

1. INTRODUCTION

The first demonstrations of terahertz imaging in biomedicine were made several years ago^{1,2} and recent advances have been made in the imaging of skin^{3,4} and teeth⁵. For most existing medical imaging techniques it is possible to estimate the feasibility of a desired imaging application in terms of radiation penetration and image contrast because data on the attenuation characteristics of human tissue are readily available. Confident prediction of the feasibility of terahertz pulsed imaging *in vivo* has been hindered because there is currently little information available about the optical properties of human tissue at terahertz frequencies, so a catalogue of these properties has been established. The data will ultimately allow estimation of the variability of the measurements, and allow estimates of penetration depth, percentage reflection at boundaries and image contrast between tissues to be made. To correspond with the ranges specified in the international guidelines for safe exposure to electromagnetic radiation^{6,7}, we define the terahertz band to comprise the wavelengths 2.6 μm to 20 mm (15 GHz to 115 THz). In this paper we present the first sets of measurements made from a range of preserved and freshly excised healthy human tissue samples. Measurements have to date been made from seven dehydrated teeth, cortical bone specimens that had been stored at 4°C from five donors and freshly excised tissue from two individuals

2. BACKGROUND

2.1. Terahertz pulsed imaging

Terahertz pulsed imaging is based on the pump and probe technique used in optical spectroscopy (Figure 1). An ultra-fast pulsed infrared laser, such as a Titanium Sapphire laser is split in two with one part used as the pump beam and the other as the probe. The pump beam is used to generate terahertz pulses, while the other forms part of the coherent detection system and is used to measure the amplitude of the terahertz electric field after interaction with the subject. There are two techniques commonly used to generate picosecond pulses of terahertz radiation. Either a voltage-biased

* e.berry@leeds.ac.uk; www.comp.leeds.ac.uk/comir/; Academic Unit of Medical Physics, University of Leeds, Wellcome Wing, Leeds General Infirmary, Great George Street, Leeds, LS1 3EX, UK.

photoconductive antenna⁸ is illuminated with pulses from the ultra-fast infrared laser, or the infrared pulses are used to illuminate a crystal having high non-linear susceptibility^{9,10}. The second technique is known as optical rectification or optical mixing and can yield pulses with frequencies up to 70 THz. The terahertz beam is collimated and focused to a spot roughly 0.5 mm in diameter using parabolic mirrors. The subject is placed at the focus of the beam. An optical delay stage is used to measure the transmitted or reflected terahertz pulse profile at a discrete number of time points, while the spatial mapping of measurements for image formation may most simply be performed using raster scanning, of either the subject or of the terahertz beam.

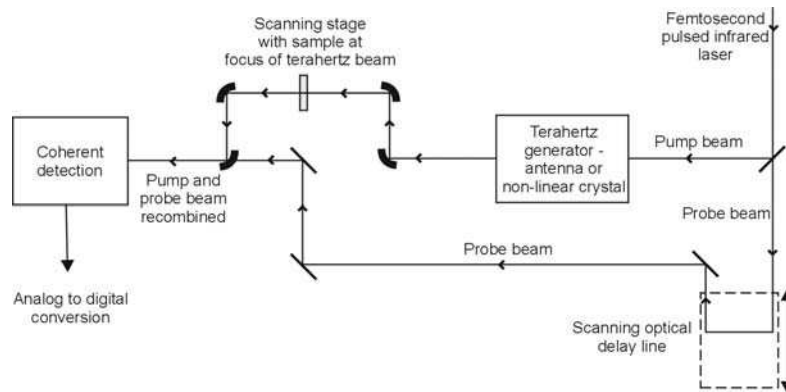


Figure 1. Schematic of a terahertz pulsed imaging system. The diagram shows an arrangement for transmission imaging. Adaptations are possible for reflection imaging and for raster scanning of the beam rather than of the sample.

Recent developments for faster image acquisition include the use of a multi-element array detector such as a charge coupled device for detection following illumination of the whole imaged area by the pump beam^{11,12}. Fuller descriptions of terahertz imaging systems may be found in^{1,13,14}. The result of the acquisition process is a 2D array comprising a time series (the pulse profile) at each point in the raster scan. The acquired pulse will be broadened and delayed compared with a reference pulse acquired without the sample in place. The changes to the pulse depend on the materials through which the pulse has been propagated and reflected. Terahertz pulsed images are parametric images, which are generated by plotting parameters derived from the measured pulse or its Fourier transform. Use of the Fourier transform, or other time frequency analysis techniques such as wavelets¹⁵ means that frequency dependent effects may be isolated. Examples of the parameters used for imaging are given in^{16,17}.

It is important to recognize the differences between terahertz systems designed for biomedical imaging and those designed for time domain spectroscopy. Spectra are acquired by both systems, but the systems differ in important ways. Spectroscopy instruments tend to be fixed pieces of laboratory instrumentation associated with other major items such as synchrotrons or free electron lasers. In contrast, systems designed for imaging in biomedicine are intended to be portable, or at least with the potential to be installed in standard hospital rooms. In spectroscopy there is no requirement for information on spatial organization in bulk tissue, and so the systems are designed to measure specially prepared samples, usually of the molecular components of tissue rather than tissue in bulk. The goal is to identify characteristic sharp molecular absorption peaks. The measurements are made at the highest spectral resolution achievable without concerns about heating the sample or acquisition time. Spectroscopic terahertz beam power could be of the order of 20 W, but the mode of terahertz generation in imaging systems means that the terahertz beam power is very much lower - currently the average power is under 1 mW. This means that in terms of hazards from heating, the imaging systems comply with existing guidelines for human exposure to electromagnetic radiation¹⁸, but a spectroscopic system may not. Spectral resolution is of lower priority in imaging, partly from pragmatic concerns about the time available for imaging, but also because it is recognized that in bulk tissue there are three confounding factors that affect the acquisition of sharp molecular absorption peaks

- Tissue samples are complex, with several molecules, which makes analysis more difficult
- In samples with many chemical environments absorption will occur over a spread of wavelengths, meaning that narrow bands do not occur
- Strong absorption by water may mask out absorption by other molecules.

It is emphasized that the spectra presented here were measured from bulk tissue on an imaging system. The spectra therefore do not have the exquisite spectral detail associated with pure molecules seen in time domain spectroscopy, but

the broadband behavior, and characteristic features seen over ranges of frequency rather than at precise frequencies, are expected to be of value.

2.2. Frequency dependent optical properties

The range of frequencies that comprises the terahertz band straddles both the region conventionally approached using optical properties (2.6 μm to 1 mm) and the region approached using dielectric properties of materials (1 mm to 20 mm). In this work we have considered the behavior to be optical in character across the full bandwidth used. This follows guidance in a recent standards document¹⁹, where exposures are considered to be quasi-optical for all wavelengths under 50mm. The changes to a terahertz pulse caused by its passage through a medium are determined by the complex refractive index of the medium, which is a function of frequency, $\tilde{n}(\omega) = n(\omega) + i\kappa(\omega)$. The complex refractive index incorporates both time delays (or phase changes in the Fourier domain) and intensity changes caused by absorption. The linear absorption coefficient, $\mu(\omega)$, is related to the imaginary part, $\kappa(\omega)$, of the complex refractive index as follows

$$\kappa(\omega) = \frac{\mu(\omega)c}{2\omega} \quad (1)$$

For addressing pulse detectability however, it is necessary first to consider the broadband optical properties for a given system (see further discussion in section 2.4), that is those measured in the time domain only using the attenuation and delay of the main pulse peak. The broadband optical properties, are not functions of frequency but do depend on the frequency make-up of the pulse, and are written here as n and μ .

Previously published articles on measurements made in the millimeter wave region describe tissue behavior in terms of dielectric rather than optical properties. To allow comparison with the measurement here, the following equations were applied to convert to refractive index $n(\omega)$ and absorption coefficient $\mu(\omega)$:

$$n(\omega) = \left[\frac{\epsilon'(\omega) + \sqrt{\epsilon'(\omega)^2 + \epsilon''(\omega)^2}}{2} \right]^{\frac{1}{2}} \quad (2)$$

$$\mu(\omega) = \frac{4\pi\omega}{c} \left[\frac{-\epsilon'(\omega) + \sqrt{\epsilon'(\omega)^2 + \epsilon''(\omega)^2}}{2} \right]^{\frac{1}{2}} \quad (3)$$

2.3. Literature overview

The definition of the terahertz band used here is 2.6 μm to 20 mm (15 GHz to 115 THz). This overlaps the region usually described as the far infrared, with wavelengths between 50 μm and 1 mm, and the region of millimeter waves which is at the extreme of the microwave region. The search for previous human tissue measurements thus included these descriptions and their synonyms, as well as "terahertz". Reports of measurements on non-human tissue were excluded.

An early paper on measurements in the terahertz band (described as far infrared by the authors) was by Barker et al in 1975²⁰. They performed a number of measurements using an incoherent detection technique, which allowed measurement of attenuation parameters but not refractive index. Although measurements of other materials were made at several wavelengths, the results presented for human bone, blood and water were measured only at 337 μm (0.9 THz). If Beer's Law is assumed, then the values found for the attenuation coefficient were respectively 39 cm^{-1} , 48 cm^{-1} , 274 cm^{-1} and 335 cm^{-1} . Note that the attenuation includes reflection and scattering losses as well as absorption, and little information appears in the article about the experimental methods used. More recent terahertz frequency work uses coherent detection, and the early reports are in the form of case studies or demonstrations with only one or two samples. Images of human tissue, prepared using standard histopathology techniques, without estimates of the optical properties, have been published by Knobloch et al^{21,22}. Cole et al³ have demonstrated reflection imaging *in vivo* of the stratum corneum epidermis boundary in the skin of the forearm and hand. The work was performed using a system giving a spectrum with its peak output at 300 GHz and a useful output up to 3 THz. It was possible to illustrate changes in hydration within the stratum corneum. Woodward et al have used reflection methods to image 15 freshly excised samples of healthy human tissue and basal cell carcinoma^{4,23,24}. This work was performed using a frequency bandwidth from 0.1 to 3.0 THz. They demonstrated differences between diseased, normal and inflamed tissue. The tissue differences could be seen on sets of images acquired 1 hour 50 minutes apart, so dehydration during this time was

not a difficulty. Some histological correlation was shown. Ciesla et al²⁵ examined human tooth enamel and dentine using a system with a frequency bandwidth from 0.5 to 2.7 THz. Measurements from a 200 μm slice gave a bulk broadband refractive index of 3.2 for enamel and 2.6 for dentine. Further work⁵ demonstrated that it was possible to measure enamel thickness accurately enough for comparative measures. In similar work on teeth, reported in the microwave literature, Hoshi et al^{26,27}, made 10 measurements of the complex permittivity of tooth enamel and dentine over a range from 0.04 to 40 GHz. Conversion to refractive index using equation (2) gives a value for healthy tooth (the average of enamel and dentine) of $n(\omega) = 2.61$ at 35 GHz. The refractive index is higher for enamel than dentine, but it is not possible to make an exact conversion from the data presented in the paper. They further compared measurements from healthy parts of each of five teeth to areas with caries. At 35 GHz the transmission coefficient though a halved tooth was lower in all cases for the caries, but it is unclear if correction for path length differences was applied.

There is an extensive literature, prompted by developments in electromagnetic dosimetry related to mobile telephony, on biological tissues at microwave frequencies. This is reviewed by Gabriel et al²⁸. In this wavelength range the behavior is described in terms of the complex dielectric properties, rather than optical properties. The bulk of the work is in the frequency range 100 MHz to 2 GHz, and on non-human tissue; but Gabriel et al include three articles on human tissue reporting measurements at frequencies above 15 GHz. The earliest is from 1950²⁹ which reports dielectric measurements made at 1.27 cm (23.6 GHz) on tissue taken from surgical operations and measured at 37 °C. The number of specimens is not given, but measurement accuracy is estimated to be better than ±10%. Conversion to refractive index using equation (2) gives values as follows for tissues that are also measured here: skin $n(\omega) = 4.97$, fat $n(\omega) = 1.87$, bone $n(\omega) = 2.52$. Alison and Sheppard³⁰ in 1993 measured the dielectric properties of blood up to 90 GHz, with $n(\omega) = 3.4$ after conversion. They found it difficult to obtain reliable measurements because of coagulation within the equipment, but their results at lower frequency were comparable with those of other authors. Since Gabriel's review, Ghodgaonkar et al³¹ have reported measurements of the complex permittivity of human skin *in vivo* in the frequency range 28-57 GHz. Measurements of the average properties of epidermis and dermis were made on only one subject; conversion to refractive index using equation (2) gives a value $n(\omega) = 2.4$ at 57 GHz. It is noted that due to differences in water content, blood content and epidermal thickness the complex permittivity (and hence refractive index) of skin *in vivo* is expected to be lower than in excised tissue.

2.4. Potential applications

With knowledge of the optical properties of various tissues it is possible to start addressing questions about imaging feasibility. The most basic question is "What thickness of tissue will reduce the signal to the level of noise?", to establish if a signal can be detected. Follow-up questions, which are not addressed here, might be "Will the primary pulse be well separated from pulses arising from multiple reflections?" and "What percentage change in optical parameters can be distinguished from normal biological variability?"

Terahertz pulsed imaging measurements are made in the time domain, and the measured pulse is the broadband response of the tissue to the range of frequencies contained in the incident pulse. Each terahertz pulsed imaging system has a unique pulse shape, which is dependent on both the characteristics of the pump laser pulse and the method used for generation of terahertz radiation. As the absorption coefficient is strongly dependent on frequency, it is expected that the broadband transmission characteristics for different terahertz pulsed imaging system will differ. Questions of detectability require the measurement of a pulse in the time domain and are therefore addressed using broadband tissue properties rather than by careful consideration of each frequency separately. Only if a pulse can be detected in the time domain is Fourier transformation possible, and at that point it is relevant to consider frequency dependent characteristics.

Simplified models of the transmission, or reflection, of a pulse through layered media can be developed using the Fresnel equations and Beer's law. The Fresnel equations (4)-(6) express the reflection and transmission coefficients at boundaries in terms of the refractive indices of the two media.

$$R_{12} = \left(\frac{n_2 - n_1}{n_2 + n_1} \right)^2 \quad (4)$$

$$T_{12} = \frac{4n_2n_1}{(n_2 + n_1)^2} \quad (5)$$

If d_2 is the distance of propagation and μ_2 is the bulk linear absorption coefficient in medium 2 for the broadband pulse, then the intensity propagation coefficient is given by

$$P_2 = \exp(-\mu_2 d_2) \quad (6)$$

The measured intensity, S after passing through the chosen construction of layered media is the incident signal intensity E multiplied by the product of the relevant values of R, T and P.

It is generally accepted that the minimum signal that is detectable is one with a value three times that of the noise³². Assuming that the noise level is the same for both incident and transmitted pulse, then the minimum detectable signal occurs when $S/E = 3/SNR$, where SNR is the signal to noise ratio of the incident pulse. Thus in each scenario, the threshold sought to determine the limit of detectability is

$$\frac{S}{E} \geq \frac{3}{SNR} \quad (7)$$

In this article we consider the basic feasibility of the following potential medical applications:

- Transmission imaging of the skin, perhaps through the web of skin in the space between thumb and first finger or a pinch on the back of the hand. This kind of measurement could have applications in the assessment of skin diseases and their treatment, and for measuring the effect of products such as moisturizers.
- Reflection imaging of the dermis epidermis boundary. Reflection imaging of skin would allow assessment of skin on any part of the body. The ability to visualize this boundary gives an indication of the depth to which features such as tumors may be seen, which is important for treatment and prognosis. Note that knowledge of depth resolution will also be required for this application.
- Transmission imaging of the tooth. It is hoped that terahertz imaging may be valuable for the detection of early caries, by helping visualization of demineralized areas. The expectation is that the microscopic porosities caused by demineralization may be detectable with terahertz pulsed imaging because they fill with saliva which is more absorbing than enamel. This is also the basis for electrical conductivity measurements³³, where the saliva forms a conducting path that would not otherwise be present.
- Reflection imaging of the enamel dentine boundary in the tooth. Again the goal would be the detection of caries. The ability to locate the enamel dentine boundary would mean that demineralized regions could be correctly assigned to lying within enamel or dentine.
- Transmission imaging, with potential for computed tomography (CT), of the distal interphalangeal (DIP) joint. Terahertz CT of the surface of a dehydrated turkey femur has recently been demonstrated^{34,35}.

In section 3.3 simple models based on the equations (4)-(6) are derived for each case, and the measured optical parameters applied. Note that a non-detectable pulse could also arise from a pulse experiencing such a large time delay that it did not arrive until after the measurement period. For the tissues considered here it was found that the absorption effects were dominant, and so delay effects have not been included in the analysis.

3. METHODS

3.1 Optical parameters

In the time domain, the attenuation of the peak pulse amplitude was measured to obtain an estimate of the broadband linear attenuation coefficient, μ . For a sample thickness x , and assuming negligible surface reflection and scattering losses, if I_0 is the incident pulse intensity, and I the transmitted pulse intensity, from the Beer-Lambert law

$$\frac{I}{I_0} = \exp(-\mu x) \quad (8)$$

where μ is the linear absorption coefficient. The influence of reflection losses was removed by making measurements at a number of different thicknesses and plotting $\ln(I/I_0)$ against thickness.

Measurements of the time delay of the peak of the pulse were used to estimate the broadband refractive index, n . For a sample thickness x , and assuming negligible surface reflection losses, if c is the velocity of light *in vacuo* then the time delay, t , for the transmitted pulse peak, is given by

$$t = \frac{(n-1)x}{c} \quad (9)$$

Measurements were made at a number of different thicknesses and t plotted against x .

In both cases, for the larger thicknesses of sample the magnitude of the transmitted signal was comparable with that of the noise. An inclusion criterion was defined so that points were only included for the determination of the slope if

$I > 0.01 I_0$. If fewer than 3 points were available, then no value was calculated. The slope and its standard deviation were found in each case using a least squares fit.

The frequency dependent linear attenuation coefficient $\mu(\omega)$ was found by assuming that the Beer-Lambert Law was valid in the frequency domain and applying equation (10)

$$\frac{I(\omega)}{I_0(\omega)} = \exp(-\mu(\omega)x) \quad (10)$$

Calculation of $n(\omega)$ is not included in this paper. The refractive index is almost constant with frequency, with a value close to the broadband refractive index.

3.2 Tissue measurements

The anonymized cortical bone samples had previously been used in a study to compare CT number and Young's modulus³⁶. Local research ethics committee approval was obtained for further use of the specimens in this work. The method used for measurement of Young's modulus meant that the bone was already cut into small beams with cross section approximately 2 x 1 mm. These proved suitable for terahertz pulsed imaging. The cortical bone specimens were harvested from five pairs of human femora and stored at -18°C before thawing for CT scanning and sample cutting, after which they were stored in saline solution at 4°C. These samples may not therefore be described as freshly excised. From a total of 180 samples, 14 have to date been measured in this work. A total of 59 single point measurements were made from the 14 bone specimens.

Local research ethics committee approval was obtained to use teeth collected in the Leeds Dental Institute for this study. Informed consent was given by patients for use of the teeth for research purposes, and the teeth were subsequently anonymized. Orthodontists prepared the teeth by cleaning out and bleaching the pulp chamber and then the tooth was autoclaved. Each tooth was sectioned in the coronal direction to obtain slices ranging in thickness from 100 to 500 μm . The slices were not rehydrated before measurement. 116 measurements were made from seven teeth as indicated in Table 1.

Tooth	slice thickness / μm	Number of enamel measurements	Number of dentine measurements	Material	Number of donors	Number of point measurements
1	80	2	0	Deionized water	Not applicable	16
2	270	11	16	Skin	2	36
3	330	12	15	Adipose tissue	2	37
4	460	8	12	Striated muscle	2	37
5	500	11	4	Vein	2	33
6	500	4	11	Artery	1	12
7	1000	5	5	Nerve	1	12

Table 1: Summary of 116 tooth samples from seven donated teeth.

Table 2: Summary of freshly excised tissue samples

Neither bone nor tooth samples were freshly excised, so local research ethics committee approval was sought and obtained for harvesting of tissue from legs amputated during vascular surgery. To date, informed patient consent has been obtained by the surgeon for the use of two such limbs, from male donors aged 64 and 71. The tissues sampled were skin, adipose tissue, striated muscle, vein, artery and nerve. Samples were placed in saline after excision and measurements were made within 48 hours of excision. No healthy artery samples were obtainable from donor 1, and measurements could not be made from the diseased tissue because of difficulties in making the samples of uniform thickness. So artery measurements were made on tissue from donor 2 only. Similarly, no nerve samples were acquired from donor 2, so nerve measurements were made on tissue from donor 1 only.

- The tooth and bone samples were held in air at the focus of the terahertz imaging system, without an enclosing medium.
- For the freshly excised tissue samples, small sections were cut to approximately the right thickness and pressed between two TPX windows separated by spacers to the required thickness: 50, 100, 150 and 200 μm . Separate reference pulses were obtained for each sample thickness by replacing the sample with an air gap of the same dimension. TPX (poly-4-methylpent-1-ene) windows were chosen because TPX has low absorption and constant refractive index over the range of frequencies of interest³⁷
- For the liquid samples, each sample was held in a polyethylene bag between two slices of polystyrene. The assembly was compressed using a mechanical translation stage to change the path length through the liquid by

known amounts, giving path length changes of 0, 25, 50, 75 and 100 μm . The reference pulses were obtained through a baseline thickness of liquid of 250 μm for water. The polystyrene was chosen because in the terahertz band it has low attenuation and a refractive index equal to that of air³⁸.

Thickness measurements for each sample at the location of measurement were made using a digital micrometer that read to $\pm 5 \mu\text{m}$. For each point measurement, a time series was recorded comprising 256 points at 80 fs intervals. This choice gave a frequency resolution of 50 GHz, a maximum frequency after Fourier transformation of 6.25 THz. The point measurements of E-field amplitude were squared to obtain intensity values. The temperature of the scanning room was maintained by air conditioning at approximately 18-20 $^{\circ}\text{C}$. The system was not purged with nitrogen, which is a technique sometimes used to reduce contributions to the spectrum from water and carbon dioxide. The following parameters were calculated from the acquired data:

- Mean and standard deviation broadband refractive index (equation (8))
- Mean and standard deviation broadband absorption coefficient (equation(9))
- Mean and standard deviation of linear absorption coefficient over frequency (equation (10)).

Two sample t-tests were performed to compare the mean values of the broadband parameters for the various tissues at the 95% level of significance.

3.3 Potential applications

3.3.1 Transmission imaging of skin

In this scenario, the pulse to be detected travels from air to skin and back to air again. For a detectable pulse, from equation (7),

$$\frac{S}{E} = T_{12}P_2T_{21} \geq \frac{3}{SNR}$$

where medium 1 is air, medium 2 is skin, and T and P are defined in equations (5)-(6). Substituting for P_2

$$d_2 \geq -\frac{1}{\mu_2} \ln \left[\frac{3}{SNR \cdot T_{12}T_{21}} \right] \quad (11)$$

where d_2 represents the thickness of skin and μ_2 the absorption coefficient of skin.

In this and in scenarios 3.2.2-3.3.4, following substitution of the measured values of refractive index and absorption coefficient, d_2 was plotted against SNR and error limits were found by evaluating the derived expression using the measured values \pm their standard deviation.

3.3.2 Reflection imaging of the dermis/epidermis boundary

In this case the pulse to be detected must travel a path from air to epidermis, through a thickness d_2 mm of epidermis, undergo reflection at the epidermis/dermis boundary, re-cross d_2 mm of epidermis and be transmitted from epidermis to air. For a detectable pulse, from equation (7)

$$\frac{S}{E} = T_{12}P_2R_{23}P_2T_{21} \geq \frac{3}{SNR}$$

where medium 1 is air, medium 2 is epidermis, medium 3 is dermis and T and P are defined in equations (5)-(6). Substituting for P_2

$$d_2 \geq -\frac{1}{2\mu_2} \ln \left[\frac{3}{SNR \cdot T_{12}R_{23}T_{21}} \right] \quad (12)$$

where d_2 represents the thickness of epidermis and μ_2 its absorption coefficient. The measured values for skin were used to represent the epidermis (medium 2) and the measured values for adipose tissue to represent dermis (medium 3).

3.3.3 Transmission imaging of the tooth

This scenario is the same as that described in section 3.3.1, but with skin replaced by tooth enamel.

3.3.4 Reflection imaging of the enamel dentine boundary in the tooth

In this case the pulse to be detected must travel a path from air to tooth enamel, through a thickness d_2 mm of enamel, undergo reflection at the enamel/dentine boundary, re-cross d_2 mm of enamel and be transmitted from enamel to air. This scenario is the same as that described in section 3.3.2, but with epidermis replaced by enamel, and dermis by dentine.

3.3.5 Transmission imaging, with potential for computed tomography, of the DIP joint

A path representing the most attenuating projection through a male adult's DIP joint was measured from an MR image to comprise 0.4 mm skin, 3.2 mm soft tissue, 1.1 mm cortical bone, 10 mm trabecular bone, 1.1 mm cortical bone, 3.2 mm soft tissue, 0.4 mm skin. For a detectable pulse

$$\frac{S}{E} = T_{12}P_2T_{23}P_3T_{34}P_4T_{45}P_5T_{54}P_4T_{43}P_3T_{32}P_2T_{21} \geq \frac{3}{SNR}$$

where medium 1 is air, medium 2 skin, medium 3 soft tissue, medium 4 cortical bone and medium 5 trabecular bone. For an initial estimate of detectability this can be reduced to a best case situation comprising a single layer of the least attenuating material, which is cortical bone. If this model is shown to allow passage of a detectable pulse, then the model may be refined to include the other components. For a single layer of cortical bone in air, the equations are the same as those used for scenario 3.3.1, but with skin replaced by cortical bone. In this case however, the equation was used simply to determine if the value of SNR required for a detectable pulse through $d_2 = 19.4$ mm was under 10000, which is a potentially attainable SNR³⁹.

4. RESULTS

4.1 Tissue measurements

Material	N_n	$\langle n \rangle$	N_μ	$\langle \mu \rangle / \text{cm}^{-1}$
Deionized water	16	2.04 ± 0.07	13	225 ± 21
Tooth enamel	44	3.06 ± 0.09	44	62 ± 7
Tooth dentine	72	2.57 ± 0.05	72	70 ± 7
Skin	36	1.73 ± 0.29	36	121 ± 18
Adipose tissue	37	1.50 ± 0.47	37	89 ± 23
Striated muscle	37	2.00 ± 0.35	37	164 ± 17
Cortical bone	59	2.49 ± 0.07	59	61 ± 3
Vein	33	1.58 ± 0.49	33	110 ± 43
Artery	12	1.86 ± 0.40	24	151 ± 25
Nerve	12	1.95 ± 0.46	12	246 ± 27

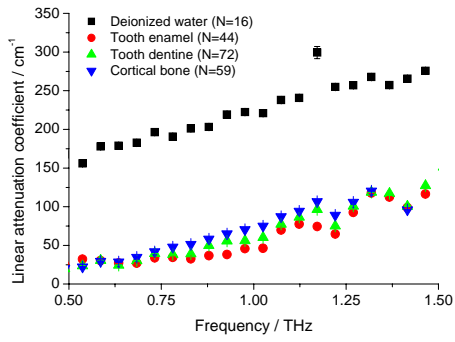
Table 3: Values for broadband refractive index (n) and broadband linear attenuation coefficient (μ). Mean values are shown \pm one standard deviation. N_n and N_μ were the number of measurements used to calculate the mean values for refractive index and linear attenuation coefficient respectively (see section 3 for the number of donors)

The broadband refractive index and attenuation coefficient results are shown in Table 3. For refractive index, the two sample t-test showed a significant difference ($P < 0.05$) between the mean values for all pairs of tissue except water and striated muscle, water and artery, water and nerve, skin and vein, skin and artery, skin and nerve, adipose tissue and vein, striated muscle and artery, striated muscle and nerve, vein and artery. For linear attenuation coefficient, the two sample t-test showed a significant difference ($P < 0.05$) between the mean values for all pairs of tissue except tooth enamel and cortical bone, skin and vein.

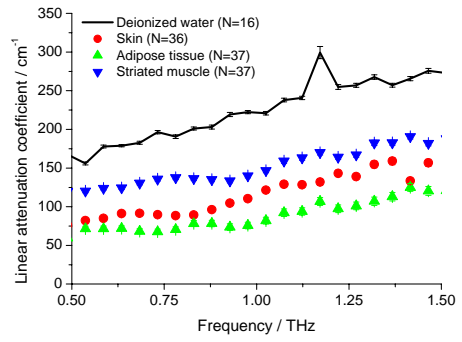
The variation of linear attenuation coefficient with frequency appears in Figure 2, the results for water are shown in all three figures for comparison. The effect of increased absorption at 1.2 THz can be clearly seen in the measurements from water. Decreased absorption at approximately the same frequency is seen for vein and nerve in Figure 2c, which may be related to increased environmental absorption affecting the reference pulse.

4.2 Potential applications

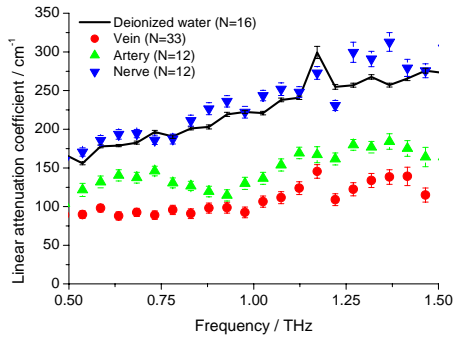
The calculated maximum thicknesses for detection of a pulse are shown in Figure 3 (a-d) for the four scenarios described in sections 3.3.1-3.3.4. Transmission imaging of the skin does not appear to be practical, but reflection imaging is more promising. For reflection imaging of the epidermis dermis boundary we made the assumption that the properties of the dermis could be represented by our measurements for adipose tissue. The reflection coefficient at such a boundary is just 0.5 %, and the effect of this is seen in the small predicted imaging depths in Figure 3b. However, the average thickness of epidermis is 0.05 to 0.15 mm⁴⁰, so the boundary will be accessible to terahertz pulsed imaging in areas of the body where the epidermis is thinner. Certainly, the stratum corneum, which may be as thin as 0.01 mm depending on location is accessible, subject to the restrictions of depth resolution. Similarly, imaging in dentistry is not ruled out by the measurements presented here in Figure 3d. For the scenario described in section 3.3.5, it was found that the necessary SNR for a detectable pulse through 19.4 mm of cortical bone was over 10000, thus terahertz CT based on projection imaging of the adult DIP joint would be infeasible using our current arrangement.



2a

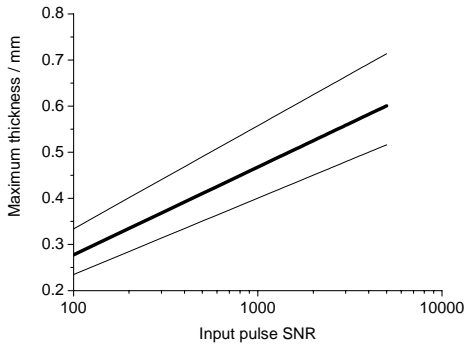


2b

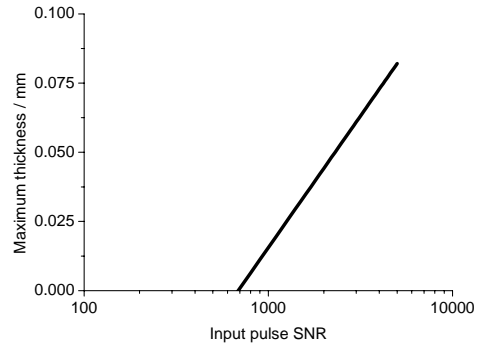


2c

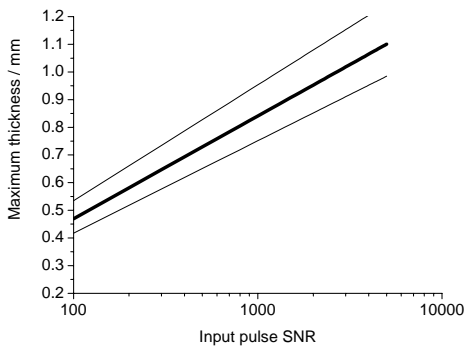
Figure 2. Measured linear attenuation coefficient as a function of frequency. Error bars indicate \pm one standard error of the mean (standard deviation/ $N^{1/2}$), N is the number of samples. a) Water, tooth enamel, tooth dentine, cortical bone b) water, skin, adipose tissue and striated muscle. c) water, vein, artery and nerve.



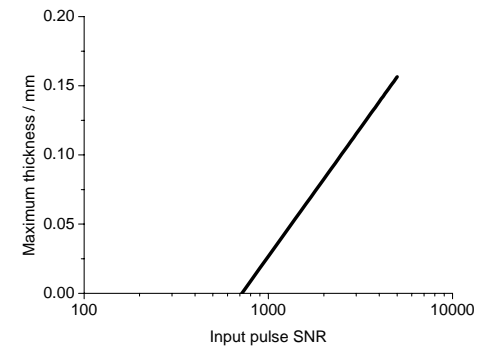
3a



3b



3c



3d

Figure 3. The calculated maximum thickness of tissue for a detectable pulse. a) transmission imaging of skin, b) reflection imaging of the epidermis/dermis boundary, c) transmission imaging of tooth enamel, d) reflection imaging of the enamel/dentine boundary.

5. CONCLUSIONS

The first systematic measurements of human tissue optical properties in the terahertz band (useful input pulse bandwidth approximately 0.5 to 2.5 THz) have been presented here. These data represent the first part of a larger study, and freshly excised samples from only two individuals have so far been included, thus the results must still be treated as preliminary. The study has some further limitations, which may affect its comparability with other work. The hydration level of tissue has a strong influence on the optical properties. The tooth samples were measured in a dehydrated condition, and future work will aim to ensure that samples are hydrated to the same degree as one another, and to maintain that hydration throughout the measurement period. The freshly excised tissue was all measured within 48 hours of excision, but was not maintained at body temperature, which will affect the results compared with values obtained *in vivo*. Whilst storage in saline prevented the samples from drying out, different tissues took up the saline in differing degrees. It has been noted⁴¹ that results from fatty tissue are strongly affected by the degree of blood infiltration, again meaning that there will be differences between excised tissue and tissue *in vivo*. The absorption coefficients presented may include attenuation due to scattering as well as absorption. A major point is that the feasibility calculations were performed using the broadband optical properties, as the method used to assess feasibility was based on the requirement that a pulse could be detected in the time domain. However, it is seen in Figure 2 that the absorption coefficient increases with frequency. For example for tooth enamel the increase over the range 0.5 THz to 1.5 THz is almost two fold. Thus systems using terahertz pulses with a different frequency composition from ours, and especially those with a higher proportion frequencies at the lower frequency end of the terahertz band, would be expected to penetrate a greater thickness of tissue. A further assumption in the feasibility calculations was that the noise level in both incident and detected pulse was the same. This assumption may have led to pessimistic estimates of detectability.

The frequency dependent absorption meant that higher frequencies in the pulse were absorbed and were rarely present in the detected pulse, a process that could be termed "beam softening". When terahertz pulsed imaging is used *in vivo*, it may be important to consider ways of removing higher frequencies before they reach the subject. It is undesirable for imaging to make use of only the low frequencies, with the higher frequencies contributing to the heating and potential damage of the tissue whilst making no contribution to the image.

The results obtained are consistent with the expected larger absorption coefficient with greater hydration. For example, in Figure 2b, the absorption coefficient of striated muscle is greater than that of adipose tissue, which is a tissue with a lower proportion of water. In Table 3, a similar difference is seen in their refractive indices. The high proportion of water in striated muscle is emphasized by the similarity of its refractive index to that of water, though their absorption coefficients differ. Similarly, the compositional relationship between tooth enamel and cortical bone can explain their similar absorption coefficients, but they do not share their refractive indices. Whilst no characteristic spectral features in the form of absorption peaks have been demonstrated, except in water, Figures 2 does show differing profiles of absorption coefficient with frequency for the different tissues. The uniqueness of these profiles, and of indices representing differences between them, is a topic for further investigation.

Regarding the refractive index of tooth enamel and dentine, the results are similar to those reported by Ciesla et al²⁵ in the terahertz band and by Hoshi et al^{26,27} at 35 GHz. The value of $n(\omega) = 1.73 \pm 0.29$ that was measured here for skin is comparable with the value of 2 assumed in the work of Cole et al³, but is lower than that measured by Ghodgaonkar et al³¹ *in vivo* at 57 GHz or the 1950 measurement at 23.6 GHz. It is likely that the better agreement for the tooth results is related to the low levels of hydration in the tooth samples, while measurements in skin are likely to vary substantially without careful control of measuring conditions. Absorption coefficient results obtained were of the same order of magnitude as the early, incoherent, measurements reported by Barker et al²⁰, and rank in the same order. Although reflection losses were included in their attenuation coefficients, the values for bone and fat are lower than those reported here, and not higher as might be expected. However, the broadband nature of our measurements, and the effect of the increased absorption seen for higher frequencies, may explain the discrepancy.

In future work, these measurements of optical properties will be used in further calculations to address questions about discriminating pathology from biological variability, optimizing the image contrast-to-noise ratio, methods for tissue differentiation using bands of frequencies and the need for index matching. An important area is modeling alternative modes of acquisition. For example, Woodward et al have demonstrated⁴, that reflection imaging may not necessarily

involve the identification of major boundaries (as in B-mode ultrasound), but instead the technique may be used to analyze reflections from within a gradually changing layer of tissue. These results will be of value in modeling this type of imaging. Similarly, it would be possible to assess the usefulness of using pulses reflected from several alternative features as references for comparison with the pulse reflected from pathology.

ACKNOWLEDGMENTS

This research was supported under the European Union Teravision Project (IST-1999-10154). Associated support was from the Engineering and Physical Sciences Research Council (GR/N39678). M Whitaker provided valuable technical support. Our thanks to SL Thornton, P Jackson, DJ Wood, F Carmichael, S Strafford, BB Seedhom, M Cuppone, R Soames, W Merchant, J Bull, M Fletcher.

REFERENCES

1. D.M.Mittleman, R.H.Jacobsen, M.C.Nuss, "T-ray imaging", *IEEE Journal of Selected Topics in Quantum Electronics*, **2**, pp. 679-692, 1996.
2. D.D.Arnone, C.M.Ciesla, A.Corchia, S.Egusa, M.Pepper, J.M.Chamberlain et al., "Applications of Terahertz (THz) technology to medical imaging", *Proceedings of SPIE Terahertz Spectroscopy and Applications II*, **3828**, pp. 209-219, 1999.
3. B.E.Cole, R.Woodward, D.Crawley, V.P.Wallace, D.D.Arnone, M.Pepper, "Terahertz imaging and spectroscopy of human skin, in-vivo", *Proceedings of SPIE: Commercial and Biomedical Applications of Ultrashort Pulse Lasers; Laser Plasma Generation and Diagnostics*, **4276**, pp. 1-10, 2001.
4. R.M.Woodward, B.E.Cole, V.P.Wallace, R.J.Pye, D.D.Arnone, E.H.Linfield et al., "Terahertz pulse imaging in reflection geometry of human skin cancer and skin tissue", *Physics in Medicine and Biology*, **47**, pp. 3853-3863, 2002.
5. D.Crawley, C.Longbottom, V.P.Wallace, B.Cole, D.Arnone, M.Pepper, "Three-dimensional Terahertz Pulse Imaging of dental tissue", *Proceedings of SPIE: Commercial and Biomedical Applications of Ultrafast and Free-Electron Lasers*, **4633**, pp. 84-89, 2002.
6. International Commission on Non-Ionizing Radiation Protection, "Guidelines on limits of exposure to laser radiation of wavelengths between 180 nm and 1,000 μm ", *Health Physics*, **71**, pp. 804-819, 1996.
7. A.Ahlbom, U.Bergqvist, J.H.Bernhardt, J.P.Cesarini, L.A.Court, M.Grandolfo et al., "Guidelines for limiting exposure to time-varying electric, magnetic, and electromagnetic fields (up to 300 GHz)", *Health Physics*, **74**, pp. 494-522, 1998.
8. D.H.Auston, K.P.Cheung, J.A.Valdmanis, D.A.Kleinman, "Coherent time-domain far-infrared spectroscopy with femtosecond pulses", *Journal of the Optical Society of America A-Optics Image Science and Vision*, **1**, pp. 1278-1278, 1984.
9. D.H.Auston, M.C.Nuss, "Electrooptic generation and detection of femtosecond electrical transients", *IEEE Journal of Quantum Electronics*, **24**, pp. 184-197, 1988.
10. X.C.Zhang, Y.Jin, B.B.Hu, X.Li, D.H.Auston, "Optoelectronic study of piezoelectric field in strained-layer superlattices", *Superlattices and Microstructures*, **12**, pp. 487-490, 1992.
11. Q.Wu, T.D.Hewitt, X.C.Zhang, "Two-dimensional electro-optic imaging of THz beams", *Applied Physics Letters*, **69**, pp. 1026-1028, 1996.
12. J.Shan, A.S.Weling, E.Knoesel, L.Bartels, M.Bonn, A.Nahata et al., "Single-shot measurement of terahertz electromagnetic pulses by use of electro-optic sampling", *Optics Letters*, **25**, pp. 426-428, 2000.
13. D.M.Mittleman, M.Gupta, R.Neelamani, R.G.Baraniuk, J.V.Rudd, M.Koch, "Recent advances in terahertz imaging", *Applied Physics B-Lasers and Optics*, **68**, pp. 1085-1094, 1999.
14. S.Mickan, D.Abbott, J.Munch, X.C.Zhang, T.van Doorn, "Analysis of system trade-offs for terahertz imaging", *Microelectronics Journal*, **31**, pp. 503-514, 2000.
15. J.W.Handley, A.J.Fitzgerald, E.Berry, R.D.Boyle, "Approaches to segmentation in medical terahertz pulsed imaging", *Proceedings of Medical Image Understanding and Analysis*, 2002, pp. 157-160, 2002.
16. A.J.Fitzgerald, E.Berry, N.N.Zinovev, G.C.Walker, M.A.Smith, J.M.Chamberlain, "An introduction to medical imaging with coherent terahertz frequency radiation", *Physics in Medicine and Biology*, **47**, pp. R67-R84, 2002.
17. T.Loffler, K.Siebert, S.Czasch, T.Bauer, H.G.Roskos, "Visualization and classification in biomedical terahertz pulsed imaging", *Physics in Medicine and Biology*, **47**, pp. 3847-3852, 2002.

18. E.Berry, G.C.Walker, A.J.Fitzgerald, N.N.Zinovev, J.M.Chamberlain, S.W.Smye et al., "Do *in vivo* Terahertz Imaging Systems comply with safety guidelines?", *Journal of Laser Applications*, In Press, 2003.
19. Institute of Electrical and Electronic Engineers, *Standard for safety levels with respect to human exposure to radiofrequency electromagnetic fields, 3 kHz to 300 GHz (IEEE C95.1 1999 Edition)*; Institute of Electrical and Electronic Engineers, New York, 1999.
20. D.H.Barker, D.T.Hodges, T.S.Hartwick, "Far infrared imagery", *Proceedings of SPIE Long Wavelength Infrared*, **67**, pp. 27-34, 1975.
21. P.Knobloch, K.Schmalstieg, M.Koch, E.Rehberg, F.Vauti, K.Donhuijsen, "THz imaging of histo-pathological samples", *Proceedings of SPIE: Hybrid and Novel Imaging and New Optical Instrumentation for Biomedical Applications*, **4434**, pp. 239-245, 2001.
22. P.Knobloch, C.Schildknecht, T.Kleine-Ostmann, M.Koch, S.Hoffmann, M.Hofmann et al., "Medical THz imaging: an investigation of histo-pathological samples", *Physics in Medicine and Biology*, **47**, pp. 3875-3884, 2002.
23. R.M.Woodward, B.Cole, V.P.Wallace, D.D.Arnone, R.Pye, E.H.Linfield et al., "Terahertz pulse imaging of *in-vitro* basal cell carcinoma samples", *Lasers and Electro-Optics, 2001 CLEO '01 Technical Digest*, pp. 329-330, 2001.
24. R.M.Woodward, V.P.Wallace, B.Cole, R.J.Pye, D.Arnone, E.H.Linfield et al., "Terahertz pulse imaging in reflection geometry of skin tissue using time domain analysis techniques", *Proceedings of SPIE Clinical Diagnostic Systems: Technologies and Instrumentation*, **4625**, pp. 160-169, 2002.
25. C.M.Ciesla, D.D.Arnone, A.Corchia, D.Crawley, C.Longbottom, E.H.Linfield et al., "Biomedical applications of Terahertz Pulse Imaging", *Proceedings of SPIE: Commercial and Biomedical Applications of Ultrafast Lasers II*, **3934**, pp. 73-81, 2000.
26. N.Hoshi, Y.Nikawa, K.Kawai, S.Ebisu, "Application of microwaves and millimeter waves for the characterization of teeth for dental diagnosis and treatment", *IEEE Transactions on Microwave Theory and Techniques*, **46**, pp. 834-838, 1998.
27. Y.Nikawa, N.Hoshi, K.Kawai, S.Ebisu, "Study on dental diagnosis and treatment using millimeter waves", *IEEE Transactions on Microwave Theory and Techniques*, **48**, pp. 1783-1788, 2000.
28. C.Gabriel, S.Gabriel, E.Corthout, "The dielectric properties of biological tissues .1. Literature survey", *Physics in Medicine and Biology*, **41**, pp. 2231-2249, 1996.
29. T.S.England, "Dielectric properties of the human body for wave-lengths in the 1-10 cm. range", *Nature*, **166**, pp. 480-481, 1950.
30. J.M.Alison, R.J.Sheppard, "Dielectric-properties of human blood at microwave-frequencies", *Physics in Medicine and Biology*, **38**, pp. 971-978, 1993.
31. D.K.Ghodgaonkar, O.P.Gandhi, M.F.Iskander, "Complex permittivity of human skin *in vivo* in the frequency band 26.5-60 GHz", *IEEE Antennas and Propagation Society International Symposium*, **2**, pp. 1100-1103, 2000.
32. D.A.Skoog, F.J.Holler, T.A.Nieman, *Principles of Instrumental Analysis*, Saunders College Publishing, 1998.
33. J.J.Ten Bosch, B.Angmarmansson, "A review of quantitative methods for studies of mineral-content of intraoral incipient caries lesions", *Journal of Dental Research*, **70**, pp. 2-14, 1991.
34. B.Ferguson, S.H.Wang, D.Gray, D.Abbot, X.C.Zhang, "T-ray computed tomography", *Optics Letters*, **27**, pp. 1312-1314, 2002.
35. B.Ferguson, S.H.Wang, D.Gray, D.Abbott, X.C.Zhang, "Towards functional 3D T-ray imaging", *Physics in Medicine and Biology*, **47**, pp. 3735-3742, 2002.
36. M.Cuppone, B.B.Seedhom, E.Berry, "The longitudinal Young's modulus of cortical bone in the midshaft of human femur and its correlation with CT scanning data", *Calcified Tissue International*, In Press, 2003.
37. M.F.Kimmitt, *Far-infrared techniques*, Pion Limited, London, 1970.
38. G.Z.Zhao, M.ter Mors, T.Wenckebach, P.C.M.Planken, "Terahertz dielectric properties of polystyrene foam", *Journal of the Optical Society of America B-Optical Physics*, **19**, pp. 1476-1479, 2002.
39. M.van Exter, D.R.Grischkowsky, "Characterization of an optoelectronic terahertz beam system", *IEEE Transactions on Microwave Theory and Techniques*, **38**, pp. 1684-1691, 1990.
40. J.Q.Lu, X.H.Hu, K.Dong, "Modeling of the rough-interface effect on a converging light beam propagating in a skin tissue phantom", *Applied Optics*, **39**, pp. 5890-5897, 2000.
41. S.Gabriel, R.W.Lau, C.Gabriel, "The dielectric properties of biological tissues .2. Measurements in the frequency range 10 Hz to 20 GHz", *Physics in Medicine and Biology*, **41**, pp. 2251-2269, 1996.